Available online at www.sciencedirect.com
ScienceDirect
Colloids and Surfaces A: Physicochem. Eng. Aspects 316 (2008) 210–216
COLLOIDS AND SURFACES A
www.elsevier.com/locate/colsurfa

Preparation and characterization of water-soluble monodisperse magnetic iron oxide nanoparticles via surface double-exchange with DMSA

Z.P. Chen [a,b,c], Y. Zhang [a,b], S. Zhang [a,b], J.G. Xia [a,b], J.W. Liu [a,b,c], K. Xu [a,b,c], N. Gu [a,b,*]

[a] State Key Laboratory of Bioelectronics, Southeast University, Nanjing 210096, PR China
[b] Jiangsu Laboratory for Biomaterials and Devices, Nanjing 210096, PR China
[c] School of Chemistry and Chemical Engineering, Southeast University, Nanjing 210096, PR China

Received 20 April 2007; received in revised form 17 August 2007; accepted 1 September 2007
Available online 12 September 2007

Abstract

A simple, but efficient method for preparation of water-soluble iron oxide nanoparticles has been developed. Monodisperse Fe_3O_4 nanoparticles were synthesized by thermal decomposition of iron-oleate. Surface double-exchange of oleic acid capped monodisperse Fe_3O_4 nanoparticles with a familiar 2,3-dimercaptosuccinnic acid (HOOC–CH(SH)–CH(SH)–COOH, DMSA) was first performed in chloroform in the presence of triethylamine, and then this process was repeated in ethanol under the same conditions. The resulting Fe_3O_4 nanoparticles could be transferred into water to form stable magnetic fluid without post-treatment processes such as filtration and re-concentration. TEM images show that water-soluble Fe_3O_4 nanoparticles remain monodisperse and even form a monolayer of ordered assembly, and the results of TGA, VSM show that Fe_3O_4 nanoparticles via surface double-exchange possess more DMSA molecules through intermolecular disulfide cross-linking between DMSA, as confirmed by Raman spectra. Zeta potential measurements show that nanoparticles after surface double-exchange are negatively charged in the range of pH = 1–14, and stability assays exhibit their excellent stability in water and other physiological environments.

Keywords: Monodisperse; Iron oxide nanoparticle; DMSA; Surface double-exchange; Water-soluble

1. Introduction

Magnetic nanoparticles have been widely studied because of their many biological applications such as magnetic separation [1,2], DNA detection [3], magnetic resonance imaging [4,5], target-drug delivery [6], and magnetic hyperthermia [7,8]. Among magnetic nanoparticles, iron oxide nanoparticles are of particular interests for applications because of their unique magnetic properties and biocompatibility. For future highly sensitive magnetic nanodevices and biological applications, iron oxide nanoparticles with controlled-shape, -size, and a narrow size distribution are urgent. Very recently, several groups have reported that such high-quality iron oxide nanoparticles could be synthesized by thermal decomposition of different types of iron precursors such as iron acetylacetonate [9], iron pentacarbonyl [10], and iron-oleate [11,12]. However, the direct products of the above-mentioned approaches are organic-soluble, which to some extent limits their applications in biological fields.

To take advantage of their high-quality properties in biological applications, it is necessary to transfer iron oxide nanoparticles from organic to aqueous solution. Some groups have reported surface modification techniques including surface exchange with cyclodextrin [13], copolypeptides [14], anionic octa(tetramethylammonium)-polyhedral oligomeric silsesquioxane (TMA-POSS) [15], and intercalation of surfactants [16]. Especially, some reports have given prominences to surface exchange with DMSA by which iron oxide nanoparticles modified are fairly stable in water over wide ranges of pH and salt concentrations [4,5,17–20], which makes them preferable in biological applications. From the point of surface chemistry, the success of any surface exchange process relies on a careful balance of the intermolecular forces driving the interaction between the molecules to be exchanged and the outermost layer of the substrate surface. Bruce et al. reported an inexpensive method for the introduction of more amino groups onto the

* Corresponding author at: State Key Laboratory of Bioelectronics, Southeast University, Nanjing 210096, PR China. Tel.: +86 25 83794960; fax: +86 25 83792576.
E-mail address: guning@seu.edu.cn (N. Gu).

0927-7757/$ – see front matter © 2007 Elsevier B.V. All rights reserved.
doi:10.1016/j.colsurfa.2007.09.017

surface of silica-coated iron oxide nanoparticles under various reaction conditions such as solvent systems and temperatures [21]. Here, we developed surface double-exchange of oleic acid capped monodisperse Fe_3O_4 nanoparticles with DMSA in the presence of triethylamine. The resulting Fe_3O_4 nanoparticles could be transferred into water to form stable magnetic fluid without post-treatment processes and kept stable for several months, even at high concentration.

2. Experimental

2.1. Materials

1-octadecene was purchased from Alfa Aesar. 4-Morpholineethanesulfonic acid (MES) was purchased from Pierce and RPMI-1640 was purchased from Gibco. Note that RPMI-1640 used in our experiments contains 10% (v/v) fetal calf serum. The other chemicals were analytical reagents and purchased from Shanghai Chemical Reagent Corporation, China. All chemicals were used as received. Distilled water was used for all the experiments.

2.2. Synthesis of monodisperse Fe_3O_4 nanoparticles

Known method was followed to synthesize monodisperse Fe_3O_4 nanoparticles [11]. Monodisperse Fe_3O_4 nanoparticles were synthesized in two steps: first, to prepare an iron-oleate precursor and second, to decompose the precursor. In a typical experiment, 2.7 g of $FeCl_3{\cdot}6H_2O$ was dissolved in 50 mL of methanol followed by addition of 8.5 mL oleic acid. And then, a solution with 1.2 g of NaOH in 100 mL of methanol was dropped into above solution under magnetic stirring conditions. The observed brown precipitate was washed with methanol 4–5 times and dried under vacuum overnight to remove all solvents. The obtained waxy iron-oleate was dissolved in 1-octadecanol at 70 °C and reserved as a stable stock solution at room temperature.

One millilitre of the above stock solution (0.39 mol/mL) was mixed with 4 mL 1-octadecanol and 0.5 mL oleic acid. The reaction mixture was heated to 320 °C at a constant heating rate of 3.3 °C/min under a nitrogen atmosphere, and then kept at that temperature for 30 min. The resulting solution was cooled and precipitated by addition of excess ethanol and centrifugation. And then, the precipitate containing Fe_3O_4 nanoparticles was washed 4–5 times with ethanol. This sample was labeled as MNP-1.

2.3. Preparation of water-soluble Fe_3O_4 via surface double-exchange

One hundred milligrams of MNP-1 was dissolved in 10 mL chloroform followed by addition of 50 μL triethylamine. Fifty milligrams of DMSA was dispersed in 10 mL dimethyl sulfoxide (DMSO). And the solution was added into the above solution containing MNP-1. The resulting solution was vortexed at 60 °C for 12 h. The solution became turbid, and the black precipitate was observed. The final sample labeled as MNP-2 was obtained by centrifugation, followed by washing with ethanol carefully, and dissolved in 10 mL water for characterization and comparison. This process was repeated, and obtained MNP-2 was dissolved in 100 mL ethanol for next reaction.

We found that MNP-2 was more easily dissolved in ethanol than water, so surface double-exchange was repeated in ethanol to introduce more DMSA molecules onto the surface of Fe_3O_4 nanoparticles. Especially, 50 μL triethylamine was added into above ethanol solution containing MNP-2, followed by addition of a solution with 50 mg DMSA in 10 mL DMSO. The solution was vortexed at 60 °C for 12 h. The final sample labeled as MNP-3 was centrifuged and washed with ethanol 4–5 times carefully. MNP-3 was collected using a permanent magnet and transferred into 10 mL water.

2.4. Characterization

The size and morphology of the particles were determined by a JEM-2000EX TEM operating at 120.0 kV. Samples were dropped, either from chloroform or water, onto a carbon-coated copper grid and dried under room temperature. IR spectra were recorded on a Nicolet Nexus 870 FT-IR spectrometer and powder samples were dried at 100 °C under vacuum for 24 h prior to fabrication of the KBr pellet. Spectra were recorded with a resolution of 2 cm^{-1}. Raman spectra were collected on a JY HR800 spectrometer with a resolution of 1 cm^{-1}. Thermogravimetric analysis (TGA) was performed for powder samples (~5 mg) with a heating rate of 20 °C/min using a Perkin-Elmer TGA 7 Thermogravimetric Analyzer in synthetic N_2 atmosphere up to 700 °C. Magnetic measurements were carried out with a Lakeshore 7470 vibrating sample magnetometer (VSM).

Photon correlation spectroscopy (PCS) was used to determine hydrodynamic size distribution using a Beckman Coulter N4 Plus Submicron Particle Analyzer, and surface charge measurements were performed with a Beckman Coulter Delsa 440SX Zeta Potential Analyzer. Furthermore, to investigate stability of MNPs dispersed in different media, 1 mL MNP-2 solution was added to four 50 mL beakers containing 50 mL water, RPMI-1640, PBS and MES buffer solution, respectively. The suspension was settled at room temperature and the upper solution was taken to record UV–visible absorbance spectra every day for 5 days [15], using a U-4100 spectrophotometer. Stability assays for MNP-3 were performed as above-mentioned process.

3. Results and discussion

3.1. TEM

Monodisperse Fe_3O_4 nanoparticles (MNP-1) were synthesized by thermal decomposition of iron-oleate in the presence of oleic acid. TEM image (Fig. 1a) shows that MNP-1 is monodisperse with about 10 nm average diameter and well-dispersed in chloroform. According to the ED pattern (Fig. 1b), the *d*-spacing can be calculated in the following equation:

$$L\lambda = dR$$

where L is the distance between the test sample and the film (L = 137 cm), λ the wavelength of electron beam (λ = 0.0251 A°)

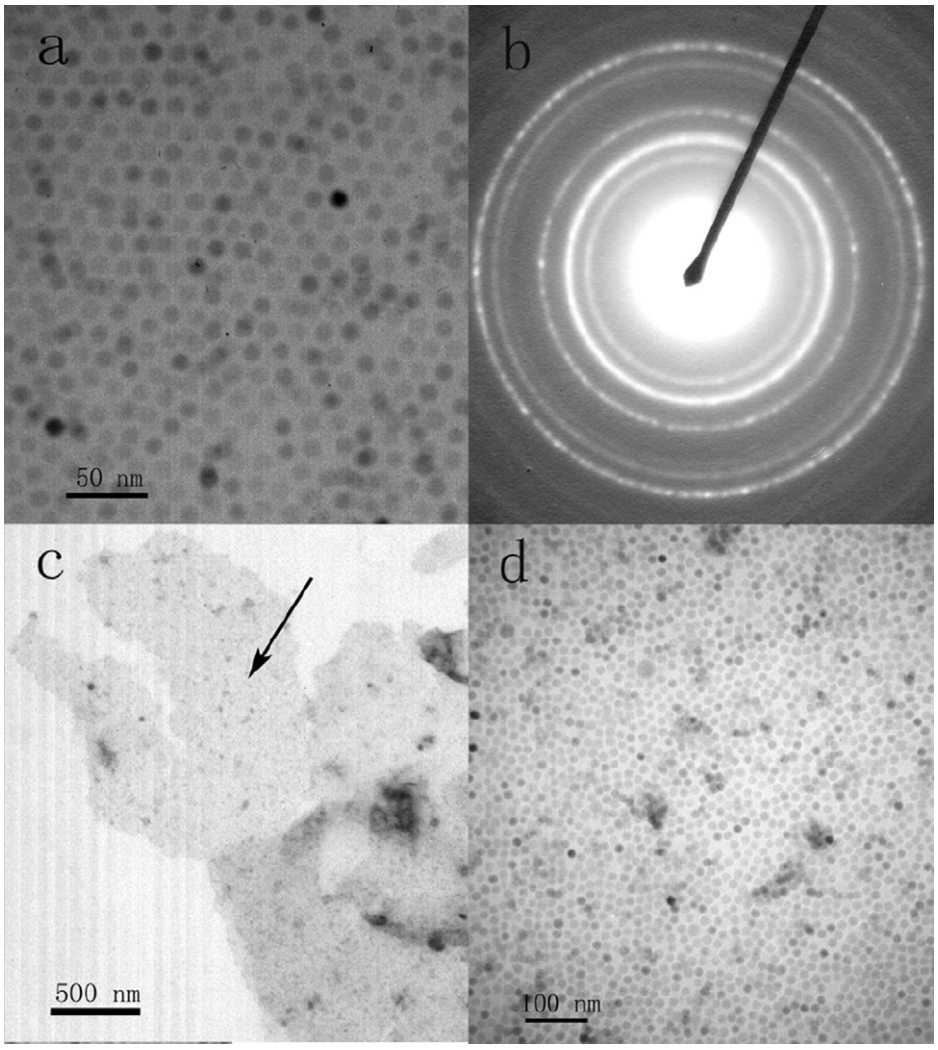

Fig. 1. (a) TEM image of MNP-1 dispersed in chloroform; (b) ED image of MNP-1; (c) TEM image of MNP-3 dispersed in water; (d) enlarged image of region marked with the arrow in (c).

and R is the radius of the diffraction ring. The calculation results are shown in Table 1, which are well accorded with theory values of the inverse cubic spinel structure of Fe_3O_4. Water-soluble Fe_3O_4 nanoparticles (MNP-3) were prepared in chloroform followed by repeated performance in ethanol via surface double-exchange with DMSA in the presence of triethylamine. TEM images (Fig. 1c and d) show that MNP-3 is well dispersed in water (the TEM image of MNP-2 is not provided because there is no obvious differences between MNP-2 and MNP-3). In addition, these images indicate that no degradation takes place upon transfer from organic to aqueous solution.

3.2. IR and Raman

IR spectra of MNP-1, MNP-2, MNP-3 and pure DMSA are shown in Fig. 2. IR spectra for all samples exhibit one interesting region located between 1800 and 1500 cm^{-1}. In spectrum a, the sharp peak at 1715 cm^{-1} assigned to carbonyl indicates that there is free oleic acid [22] and the two peaks at 1569 and 1519 cm^{-1} due to the symmetric and asymmetric carboxylate (COO^-) stretch, respectively, indicate that oleic acid is bound to the surface of Fe_3O_4 nanoparticles through covalent bond between carboxylate (COO^-) and Fe atom [23–25]. The appearance of a broad peak at 1580 cm^{-1} in spectrum b and two broad

Table 1
ED experimental data of MNP-1 in comparison with theory values

	1	2	3	4	5	6	7
R (cm)	0.70	1.16	1.36	1.64	2.01	2.12	2.32
ED results, d (Å)	4.89	2.95	2.52	2.09	1.70	1.62	1.48
Theory values, d (Å)	4.85	2.97	2.53	2.10	1.71	1.62	1.48
Crystalline lane (hlk)	(1 1 1)	(2 2 0)	(3 1 1)	(4 0 0)	(4 2 2)	(5 1 1)	(4 4 0)

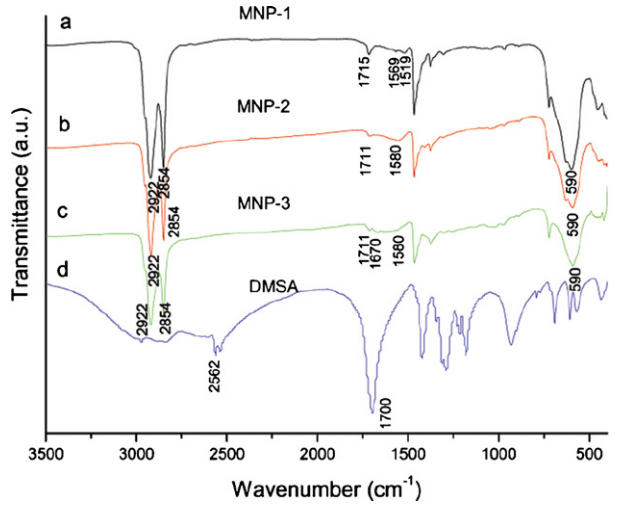

Fig. 2. IR spectra of (a) MNP-1, (b) MNP-2, (c) MNP-3 and (d) DMSA.

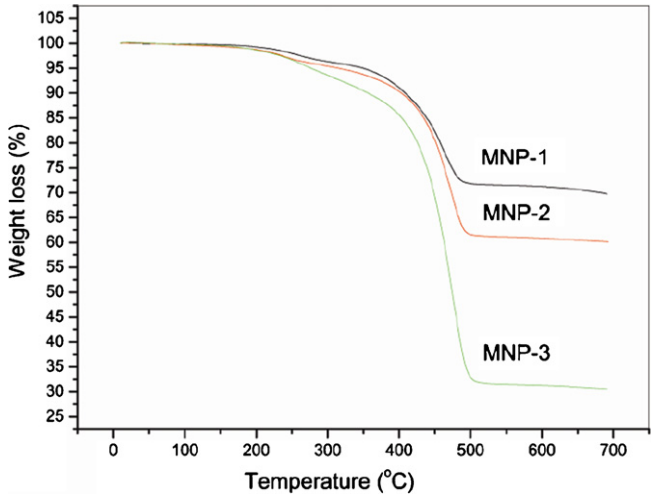

Fig. 4. TGA curves of MNP-1, MNP-2 and MNP-3.

peaks at 1670 and 1580 cm^{-1} in spectrum c derived from the symmetric and asymmetric stretch of carboxylate (COO^-) of DMSA indicates that DMSA is bound to the surface of Fe_3O_4 nanoparticles. In spectrum d, the weak peak at 2562 cm^{-1} is attributed to thiol group and the sharp peak at 1700 cm^{-1} is assigned to the carbonyl stretch of DMSA as a diacid. Therefore, the appearance of the low frequency of the peak at 1711 cm^{-1} both in spectra b and c, compared to the frequency for free oleic acid (1715 cm^{-1}), is attributed to free carbonyl stretch of DMSA on the surface of Fe_3O_4 nanoparticles. Additionally, the presence of the sharp methylene peaks at 2922 and 2854 cm^{-1}, in spectra a–c, indicates that some of initial oleic acid remains on the surface of Fe_3O_4 nanoparticles after modification. The reason of the lack of evidence of thiol group and disulfide group, in spectra b and c, is that most of thiol groups have been oxidated into disulfide groups which are lower absorption in IR analysis. So Raman spectra are used to confirm disulfide groups, as shown in Fig. 3. No peak is observed for MNP-1 between 300 and 800 cm^{-1}, whereas a sharp peak for MNP-3 appears at about 503 cm^{-1},

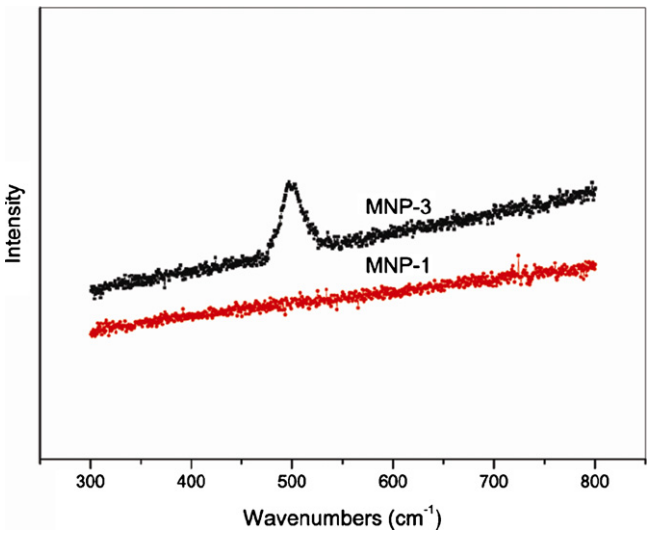

Fig. 3. Raman spectra of MNP-1 and MNP-3.

due to strong absorption of disulfide groups. This result suggests that intermolecular disulfide cross-linking between DMSA molecules can introduce more DMSA molecules onto the surface of nanoparticles.

3.3. TGA

TGA has been performed to confirm the coating formation and estimate the binding efficiency on the surface of Fe_3O_4 nanoparticles. Fig. 4 shows the weight loss for MNP-1, MNP-2 and MNP-3. A slight weight loss is observed up to 250 °C in all curves, probably due to adsorbed water, while a significant weight loss takes place between 250 and 500 °C. The weight loss for MNP-1, attributed to decomposition of oleic acid, is about 25%, corresponding to a monolayer of oleic acid on the surface [26]. The weight loss for MNP-2 and MNP-3 is increased to 34% and 65%, respectively, mainly due to the decomposition of DMSA. Interestingly, the molecular weights of oleic acid and DMSA are 282 and 182, respectively. Assuming one DMSA molecule exchanged with one oleic acid molecule, the weight loss for both of MNP-2 and MNP-3 should be 13.6% in contrast with MNP-1, while if one DMSA molecule exchanged with two oleic acid molecules, the weight loss for them should be 7.8%. Therefore, the increased weight loss for MNP-2 and MNP-3 suggests that a multilayer of DMSA exists on their surfaces. Especially, the more significant weight loss for MNP-3 than MNP-2 (69%:39%) shows that more DMSA molecules exist on the surface of MNP-3.

3.4. Magnetic measurements

Magnetic measurements indicate superparamagnetic behavior at room temperature for all samples, with no hysteresis and perfect Langevin behavior (Fig. 5). The saturation magnetization value (M_s) for MNP-1 is 50.2 emu/g, while the M_s for MNP-2 and MNP-3 are decreased to 33.4 and 16.6 emu/g, respectively. There are several approaches that can explain the reduction of the M_s for coated magnetic nanoparticles [27–29]. In this case,

Table 2
The M_S for Fe_3O_4 cores based on TGA and VSM results

Sample	Percentage of Fe_3O_4 core (% determined by TGA)	Total M_S (emu/g; determined by VSM)	The M_S of Fe_3O_4 core (emu/g)
MNP-1	72	50.2	69.72
MNP-2	61	33.4	54.75
MNP-3	31	16.6	53.55

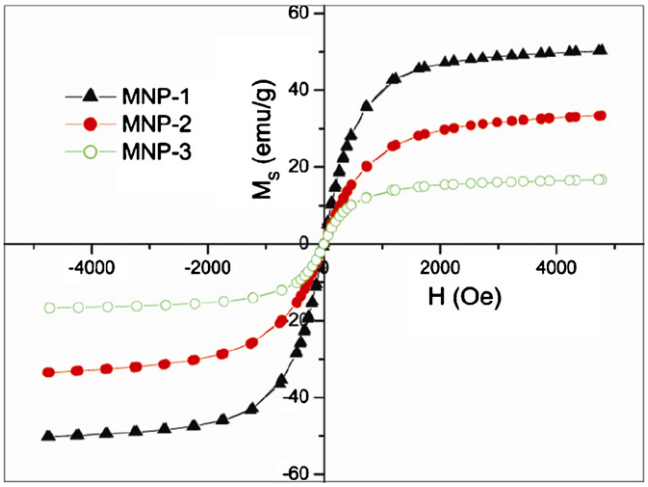

Fig. 5. Hysteresis loops at room temperature for MNP-1, MNP-2 and MNP-3.

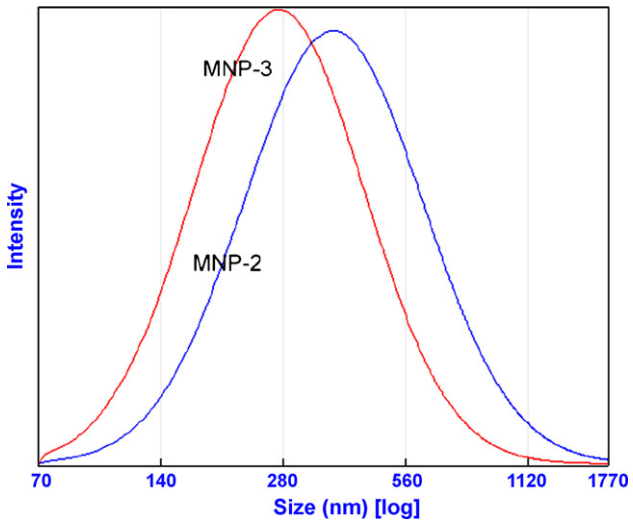

Fig. 6. Hydrodynamic size distribution of MNP-2 and MNP-3 dispersed in water.

the presence of nonmagnetic DMSA molecules on the surface of MNP-2 and MNP-3 leads to decrease of the M_S, and more decrease of the M_S for MNP-3 than MNP-2 indicates that there are more nonmagnetic DMSA molecules on the surface of MNP-3, which is consistent with TGA results. Furthermore, since the weight percentage for Fe_3O_4 core is about 72%, 61%, 31%, determined by TGA, the M_S for Fe_3O_4 cores of MNP-1, MNP-2 and MNP-3 are 69.72, 54.75, and 53.55 emu/g, respectively (Table 2).

3.5. Stability assays

Fig. 6 shows hydrodynamic size distribution of MNP-2 and MNP-3. The average hydrodynamic sizes of MNP-2 and MNP-3 are about 250 and 320 nm, respectively, indicating that both of MNP-2 and MNP-3 exist as aggregates in water. However, smaller hydrodynamic size of MNP-3 than MNP-2 suggests that MNPs-3 be of better stability. Zeta potential results (Fig. 7) show that MNP-3 is always negatively charged in the range of pH 1–14, whereas MNP-2 has an isoelectric point (IEP) at pH 1.62, indicating that total charge of DMSA molecules on the surface keeps MNP-3 sterically and electrically stable in water.

Many biological applications require magnetic nanoparticles to exhibit stability in physiological environments, so we investigate stability of MNP-2 and MNP-3 in water, RPMI-1640 (a complex medium for cell culture) and two kinds of buffer solutions (MES and PBS) based on UV–visible absorbance (Fig. 8). After settling for 5 days, for MNP-2 dispersed in water, MES, PBS, UV–visible absorbance changes from 0.294, 0.303 and 0.31 to 0.089, 0 and 0, respectively (Fig. 8a). While for MNP-3, it changes from 0.289, 0.303 and 0.306 to 0.168, 0.101 and 0.12, respectively (Fig. 8b). These results indicate that MNP-3 is more stable than MNP-2 in water and physiological environments. Interestingly, UV–visible absorbance of MNP-2 dispersed in RPMI-1640 changes to 0 after 5 days, indicating that there are almost no Fe_3O_4 nanoparticles in the upper solution. However, UV–visible absorbance of MNP-3 dispersed in RPMI-1640 changes from 0.328 to 0.251, indicating that it is the most stable for all the samples.

3.6. Structure and water-solubility test

In our surface double-exchange reactions, DMSA is used to exchange with long-chain oleic acid on the surface of Fe_3O_4

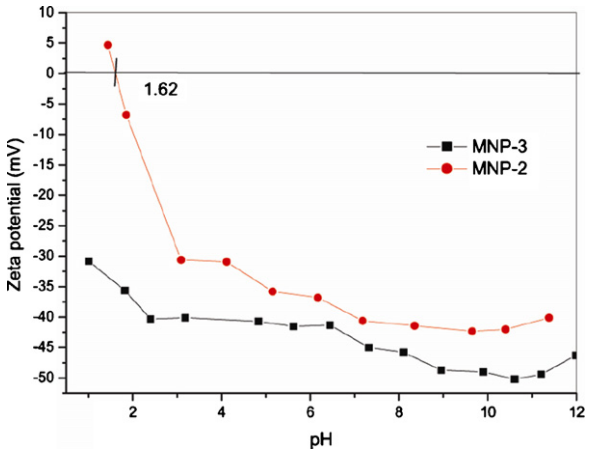

Fig. 7. Zeta potentials of MNP-2 and MNP-3.

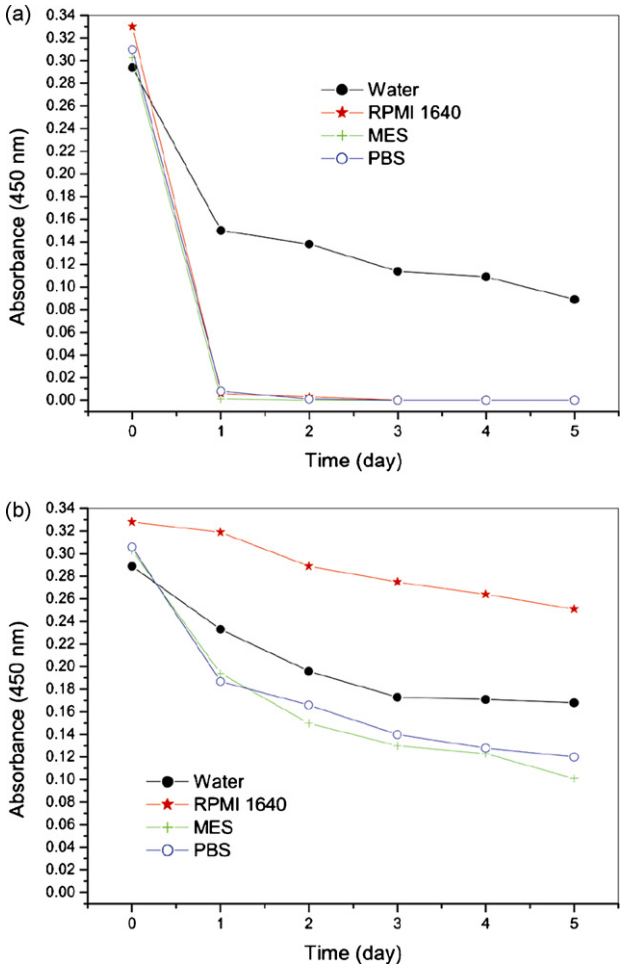

Fig. 8. Stability assays of MNP-2 (a) and MNP-3 and (b) dispersed in water, RPMI-1640 (pH 7.0), PBS (pH 7.4) and MES buffer solution (pH 4.9), respectively.

nanoparticles. Furthermore, it is noticeable that alkalescent triethylamine plays an important role as catalyst. It can deprive of hydrogen ions of carboxyl of DMSA to form carboxylate which is preferable to exchange with long-chain oleic acid. The surface double-exchange reaction without triethylamine was carried out for comparison, and we found that the resulting Fe_3O_4 nanoparticles were not stable in water at high concentration (data not provided). DMSA is exchanged onto the surface of nanoparticles by at least one carboxyl. DMSA first forms a stable coating through its carboxylic chelating bonding and further stability is obtained through intermolecular disulfide cross-linking between DMSA molecules. The remaining carboxylates ensure surface charges and can be used for conjugating with biological molecules and further applications. Fig. 9a is schematic illustration for the structure of Fe_3O_4 nanoparticles modified by DMSA. We consider that the difference between MNP-2 and MNP-3 is the amount of DMSA on the surface of Fe_3O_4 nanoparticles, as confirmed by TGA, VSM and water-solubility test (Fig. 9b). Although no precipitate is observed when both of MNP-2 and MNP-3 are dispersed in water at the high concentration of 10 mg/mL, MNP-2 is precipitated thoroughly and MNP-3 remains stable after 10 days, which

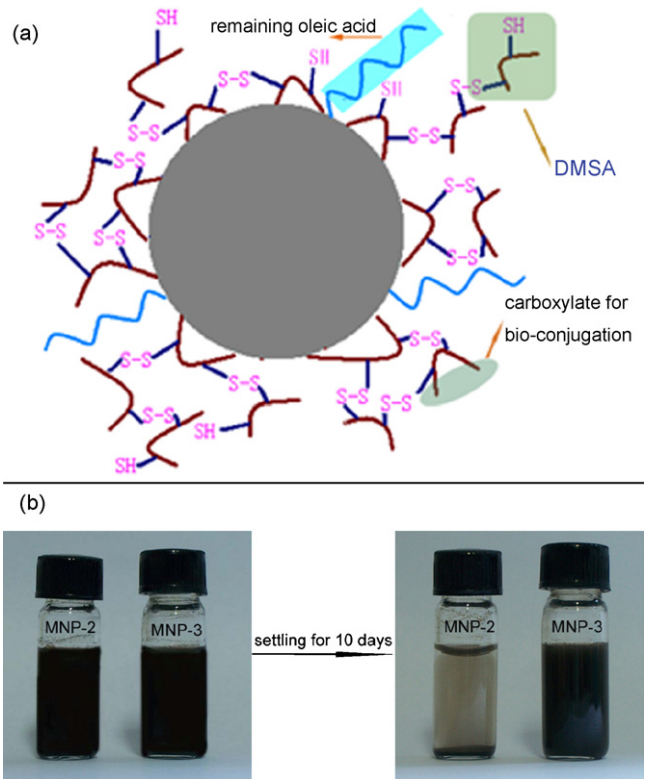

Fig. 9. (a) Schematic illustrations for the structure of MNP-2 and MNP-3 and (b) water-solubility test of MNP-2 and MNP-3.

indicates that the surface of MNP-3 possesses more DMSA molecules.

4. Conclusions

Oleic acid capped monodisperse Fe_3O_4 nanoparticles have been successfully transferred into aqueous solution via surface double-exchange with DMSA in the presence of triethylamine. The characterization results show that surface double-exchange is an efficient method that can introduce more DMSA molecules onto the surface of nanoparticles through intermolecular disulfide cross-linking between DMSA. By this means, we obtain stable nanoparticles with negative charges in the range of pH = 1–14. Moreover, the resulting products can be dispersed in water and other physiological solutions. Because DMSA is a nontoxic and biocompatible product used in many applications, high-quality magnetic nanoparticles modified by DMSA by this means may be promising in biologically relevant applications.

Acknowledgments

This work has been carried out under financial support of the National Natural Science Foundation of China (Nos. 60571031, 60501009 and 90406023) and National Basic Research Program of China (Nos. 2006CB933200 and 2006CB705600). The author would like to thank Mr. A.Q. Xu, from the Analysis and Testing Centre of Southeast University for technique assistances.

References

[1] J.P. Dailey, J.P. Phillips, C. Li, et al., J. Magn. Magn. Mater. 194 (1999) 140.
[2] A. Jordan, R. Scholz, P. Wust, et al., J. Magn. Magn. Mater. 194 (1999) 185.
[3] L. Josephson, J.M. Perez, R. Weissleder, Angew. Chem. Int. Ed. 40 (2001) 3204.
[4] Y.-M. Huh, Y.-W. Jun, H.-T. Song, et al., J. Am. Chem. Soc. 127 (2005) 12387.
[5] Y.-W. Jun, Y.-M. Huh, J.-S. Choi, et al., J. Am. Chem. Soc. 127 (2005) 5732.
[6] T.K. Jain, M.A. Morales, S.K. Sahoo, et al., Mol. Pharm. 2 (2005) 194.
[7] A. Jordan, R. Scholz, P. Wust, et al., J. Magn. Magn. Mater. 201 (1999) 413.
[8] R.Z. Xu, Y. Zhang, M. Ma, et al., IEEE Trans. Magn. 43 (2007) 1078.
[9] S. Sun, H. Zeng, J. Am. Chem. Soc. 124 (2002) 8204.
[10] T. Hyeon, S.S. Lee, J. Park, et al., J. Am. Chem. Soc. 123 (2001) 12798.
[11] N.R. Jana, Y. Chen, X. Peng, Chem. Mater. 16 (2004) 3931.
[12] J. Park, K. An, Y. Hwang, et al., Nat. Mater. 3 (2004) 891.
[13] Y. Wang, J.F. Wong, X. Teng, et al., Nano Lett. 3 (2003) 1555.
[14] L.E. Euliss, S.G. Grancharov, S. O'Brien, et al., Nano Lett. 3 (2003) 1489.
[15] B.L. Frankamp, N.O. Fischer, R. Hong, et al., Chem. Mater. 18 (2006) 956.
[16] T. Pellegrino, L. Manna, S. Kudera, et al., Nano Lett. 4 (2004) 703.
[17] N. Fauconnier, J.N. Pons, J. Roger, et al., J. Colloid Interface Sci. 194 (1997) 427.
[18] M. Auffan, L. Decome, J. Rose, et al., Environ. Sci. Technol. 40 (2006) 436.
[19] F. Bertorelle, C. Wilhelm, J. Roger, et al., Langmuir 22 (2006) 5385.
[20] M.P. Garcia, R. Miranda Parca, S. Braun Chaves, et al., J. Magn. Magn. Mater. 293 (2005) 277.
[21] I.J. Bruce, T. Sen, Langmuir 21 (2005) 7029.
[22] A.L. Willis, N.J. Turro, S. O'Brien, Chem. Mater. 17 (2005) 5970.
[23] L. Zhang, R. He, H. Gu, Appl. Surf. Sci. 253 (2006) 2611.
[24] Y. Ren, K.-I. Iimura, T. Kato, Langmuir 17 (2001) 2688.
[25] Z. Li, L. Wei, M.Y. Gao, et al., Adv. Mater. 17 (2005) 1001.
[26] A.G. Roca, M.P. Morales, K. Grady, et al., Nanotechnology 17 (2006) 2783.
[27] T. Sato, T. Iijima, M. Seki, et al., J. Magn. Magn. Mater. 65 (1987) 252.
[28] J. Popplewell, L. Sakhnini, J. Magn. Magn. Mater. 149 (1995) 72.
[29] M. Mikhaylova, D.K. Kim, C.C. Berry, et al., Chem. Mater. 16 (2004) 2344.